$$= \int_o^\infty c_o(\theta) \exp - k\theta \, d\theta$$

$$= \int_o^\infty c_o(t) \exp - \frac{k}{\tau} t \frac{1}{\tau} dt$$

$$= \frac{1}{\tau} \int_o^\infty c_o(t) \exp - k't \, dt = \frac{1}{\tau} \alpha_o \qquad (A\text{-}14)$$

where

$$k' = \frac{k}{\tau} \qquad (A\text{-}15)$$

Similarly

$$I(o) = \frac{1}{\tau} \int_o^\infty c_i(t) \exp - k't \, dt = \frac{1}{\tau} \alpha_i \qquad (A\text{-}16)$$

$$0'(o) = \frac{1}{\tau^2} \int_o^\infty t \, c_o(t) \exp - k't \, dt = \frac{1}{\tau^2} \beta_o \qquad (A\text{-}17)$$

$$I'(o) = \frac{1}{\tau^2} \int_o^\infty t \, c_i(t) \exp - k't \, dt = \frac{1}{\tau^2} \beta_i \qquad (A\text{-}18)$$

From Equation (A-11)

$$T(o) = \exp \frac{N_{Pe} - \sqrt{N^2_{Pe} + 4N_{Pe} k'\tau}}{2} \qquad (A\text{-}19)$$

$$T'(o) = \frac{N_{Pe}}{\sqrt{N^2_{Pe} + 4N_{Pe} k'\tau}} \exp \frac{N_{Pe} - \sqrt{N^2_{Pe} + 4N_{Pe} k'\tau}}{2} \qquad (A\text{-}20)$$

By substituting (A-14), (A-16), and (A-19) into (A-12), there results

$$A = \frac{\alpha_o}{\alpha_i} = \exp \frac{N_{Pe} - \sqrt{N^2_{Pe} + 4N_{Pe} k'\tau}}{2} \qquad (A\text{-}21)$$

and by substituting appropriately into (A-13), there results

$$B = \frac{\beta_o}{\alpha_o} - \frac{\beta_i}{\alpha_i} = \frac{\tau N_{Pe}}{\sqrt{N^2_{Pe} + 4N_{Pe} k'\tau}} \qquad (A\text{-}22)$$

By solving (A-21) and (A-22) simultaneously for τ and N_{Pe}, one obtains

$$\tau = \frac{2B \ln A}{2 \ln A + 4Bk} \qquad (A\text{-}23)$$

$$N_{Pe} = \frac{2 \ln A}{1 - \frac{\tau}{B}} \qquad (A\text{-}24)$$

Thus, to compute τ and N_{Pe} from the data one computes the zeroth and first moments of the modified function $c \exp - k'\tau$ at each of the measurement points. One then computes A and B according to Equations (A-21) and (A-22) and then τ and N_{Pe} from Equations (A-23) and (A-24).

Manuscript received January 24, 1966; revision received May 18, 1966; paper accepted May 20, 1966.

Interfacial Turbulence During the Absorption of Carbon Dioxide into Monoethanolamine

P. L. T. BRIAN, J. E. VIVIAN, and D. C. MATIATOS

Massachusetts Institute of Technology, Cambridge, Massachusetts

Severe discrepancies exist between theoretical considerations and the carbon dioxide–monoethanolamine absorption data available in the literature. By desorbing the inert tracer propylene simultaneously with the absorption of carbon dioxide into monoethanolamine in a short wetted-wall column, it is shown that the physical mass transfer coefficient is increased substantially by the carbon dioxide–monoethanolamine chemical absorption process. This is presumably due to interfacial turbulence driven by surface tension gradients. The use of the actual physical mass transfer coefficient prevailing during carbon dioxide absorption into monoethanolamine results in a considerable improvement in the agreement between the penetration theory solution and the experimental data on the rate of absorption of carbon dioxide into monoethanolamine.

During the past twenty years a considerable amount of research has been directed toward understanding the effect of a simultaneous liquid phase chemical reaction upon the rate of gas absorption. Theoretical studies have been based upon the use of idealized models of the absorption process, and the differential equations describing these models have been solved for various types of chemical reaction mechanisms and reaction kinetic equations. These theoretical studies have been supplemented by a number of experimental investigations with the use of laboratory absorbers, such as the short wetted-wall column and the laminar liquid jet, in which the interfacial area is known accurately and in which physical absorption rates have been shown to agree closely with penetration theory predictions.

In a few instances, encouraging quantitative agreement has been achieved between the theoretical predictions and the experimental measurements of the rate of gas absorption accompanied by a simultaneous chemical reaction. There have, however, been a number of disturb-

TABLE 1. REACTION RATE CONSTANT

T, °C.	k_F, liters/(g.-mole)(sec.)
18	5,100
25	7,600
35	9,700

ing instances in which the experimental data were found to deviate sharply from the theoretical predictions. A prominent example is the absorption of carbon dioxide into aqueous monoethanolamine (MEA) solutions.

Four sets of experimental data on the rate of absorption of carbon dioxide into aqueous monoethanolamine solutions in laminar jet and short wetted-wall column absorbers are available. Some of these data appear, upon casual observation, to agree with theoretical predictions. Astarita et al. (*6*) concluded that the reliability of classical chemical absorption theory for this system had been proved and that the system was quite well understood. Similarly, in the recent edition of "Chemical Engineers' Handbook" (*31*) Emmert and Pigford state that their data on this system are in approximate agreement with theory. However, when the various sets of experimental data on the rate of absorption of carbon dioxide into monoethanolamine solutions are compared critically with each other and with theory, severe and baffling disagreements are evident.

PREVIOUS EXPERIMENTAL RESULTS

The absorption of carbon dioxide into aqueous MEA is a liquid phase controlled process, with no appreciable gas phase resistance to the transfer, and according to several investigators (*6, 7, 11, 37*) the main chemical reaction occurring in the liquid phase is

$$CO_2 + 2\,HOCH_2CH_2NH_2 \rightarrow HOCH_2CH_2NHCOO^- + HOCH_2CH_2NH_3^+ \quad (1)$$

with a chemical kinetic rate equation given by

$$\text{Reaction rate [moles/(sec.)(liter)]} = k_F A B \quad (2)$$

Reaction (1) presumably occurs in two steps. First, one molecule of amine reacts with one molecule of carbon dioxide to form carbamic acid. The carbamic acid ionizes and the hydrogen ion then reacts with a second amine molecule to form the ammonium ion. The second step, a proton transfer, is generally believed to be much faster than the first step. Thus the net effect can be described (*9*) by the overall reaction, Equation (1), with the kinetic expression for the first step, Equation (2). Therefore, the theoretical solution to which the experimental data will be compared is the penetration theory for a second-order reaction (*8, 10*) with a stoichiometric coefficient ν equal to 2. The theoretical result is expressed as ϕ vs. $\sqrt{M}$ for various values of q. For a value of the diffusivity ratio r equal to 0.573, which corresponds to the published diffusion coefficients (*19, 42*) for carbon dioxide and MEA, the penetration theory solution has been approximated to within 3 to 5% by use of the correlation in reference *8*, and the result is given by the curves in Figures 1 through 6 and in Figures 8, 9, 13, and 14.

Before comparing experimental results with the theory, the value of the reaction rate constant k_F must be known in order to compute $\sqrt{M}$ for the experimental data. Table 1 shows values of k_F reported by Sharma (*36*). These were obtained from liquid jet absorption data, presumably under pseudo first-order reaction conditions, but the detailed data are not given by that author. However, it is encouraging that the rate constant at 18°C. obtained by Sharma is only 8% larger than the one obtained by a different method by Jensen, Jørgensen, and Faurholt (*20*). In view of this agreement, the rate constants in Table 1 are employed here.

Clarke (*11*) has reported data on the rate of absorption of carbon dioxide into MEA solutions in a laminar liquid jet at 25°C. A pure carbon dioxide gas phase was employed at pressures of 0.1 and 1 atm. Figure 1 shows a comparison of Clarke's data with the penetration theory curves. The points shown are not actual data points but rather represent the range of Clarke's experimental data, and the actual data points at any concentration would lie on a straight line drawn through the corresponding pair of points in Figure 1.

It can be seen in Figure 1 that Clarke's data agree well with the pseudo first-order curve, that is, the theoretical curve for $q = \infty$. Thus it may be presumed that Clarke's data are in agreement with the unreported laminar jet absorption data from which Sharma (*36*) obtained the k_F values listed in Table 1. However, an examination of Figure 1 reveals that all of Clarke's data should not agree with the pseudo first-order curve. For example, the theoretical curve for $q = 24.6$ falls about 25% below the pseudo first-order curve at $\sqrt{M} = 13$, but the experimental results do not show this trend. Similar although smaller deviations are observed for the other results at $p = 1$ atm. Clarke mentioned these discrepancies in his paper (*11*).

Figure 2 shows some data of Astarita (*1, 4, 5*) compared with the theoretical predictions. These data were obtained in Italy and shall be referred to as Astarita's Italian data. Only a few representative data points are shown on the plot. They were obtained at 21.5°C. with a laminar liquid jet. Astarita concluded that for this temperature $k_F = 5{,}400$ liters/(g.-mole)(sec.). This value is only 13% lower than Sharma's results, and consequently it was retained in computing the results shown in Figure 2.

It can be seen in Figure 2 that Astarita's data fall above the theoretical curves, the deviation being as much as a factor of 1.8 for the lowest amine concentration. The experimental ϕ values are so high that they exceed the theoretical asymptotes ϕ_a; thus the data conflict with the

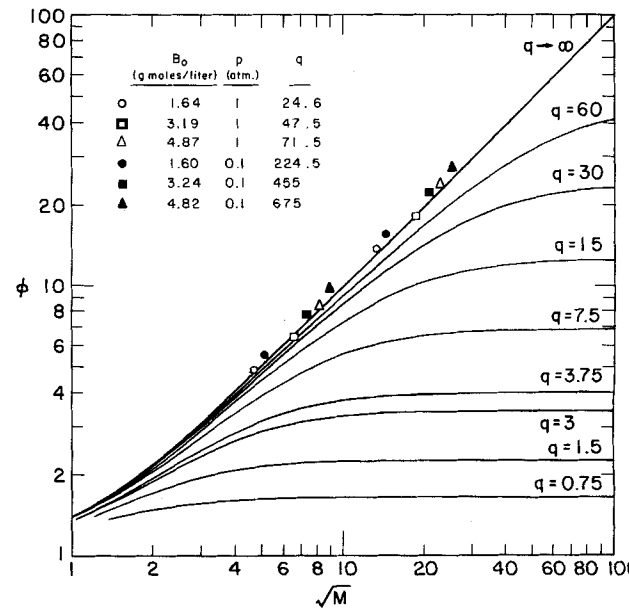

Fig. 1. Clarke's data.

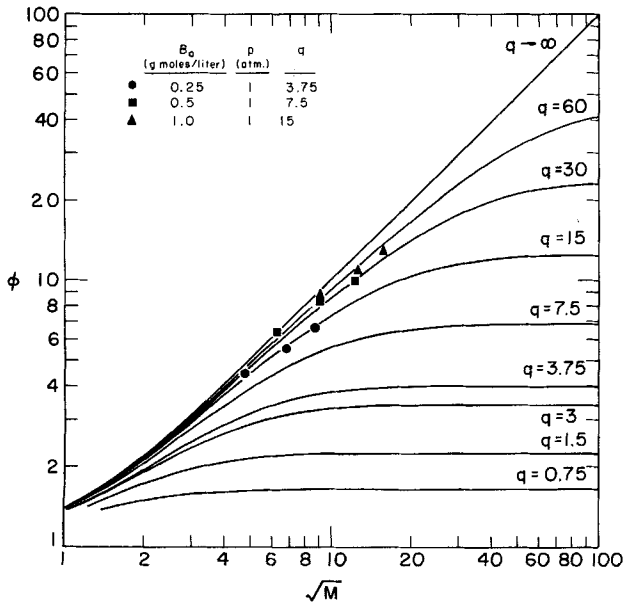

Fig. 2. Astarita's Italian data.

theory no matter what value of k_F is chosen for computing $\sqrt{M}$. Indeed, the data would still be above the theoretical curves even if it was assumed that the stoichiometric coefficient ν is equal to one molecule of amine consumed for each carbon dioxide molecule. This would correspond (9) to assuming that the second step of the two-step chemical reaction mechanism is very slow instead of very fast. In this case, the values of q for the experimental points would become twice the values reported in Figure 2, but even then the data would still lie above the theoretical curves.

Some representative data of Emmert and Pigford (*14* to *16*) are shown in Figure 3. They were obtained with a short wetted-wall column at 25°C. Three characteristics of these results are especially noteworthy. First, for results at fixed values of B_o and A_i, ϕ is occasionally seen to be decreasing as $\sqrt{M}$ increases. This led Brian and Beaverstock (9) to observe that such behavior is to be expected if the second step of a two-step chemical reaction is slow, and to suggest that perhaps the carbon dioxide–MEA chemistry is not as described by Equations (1) and (2). Subsequent considerations will show that this is not the explanation for Emmert and Pigford's data showing ϕ decreasing as $\sqrt{M}$ increases. A second feature of the data is that results for different values of B_o and A_i but for the same ratio, q, do not describe a single curve of ϕ vs. $\sqrt{M}$ as the theory predicts. Finally, the experimental ϕ values exceed the theoretical predictions by as much as a factor of 2.3. Indeed, with $B_o = 0.1$ molar and $p = 1$ atm., ϕ exceeds ϕ_a even if ν is assumed to be 1 instead of 2.

The fourth available set of data is again due to Astarita (3), and it was obtained earlier chronologically than the Astarita Italian data discussed previously. These data shall be referred to as Astarita's American data, since they were obtained in the United States. These data were taken at 25°C. with a laminar liquid jet, and some representative results based on Sharma's rate constant are shown in Figure 4. It can be seen that the data all lie appreciably above the pseudo first-order curve, which is the upper bound for ϕ. Astarita has subsequently referred (*1, 4, 5*) to these data as representing ϕ_a values, that is, asymptotic values of ϕ for an infinitely rapid chemical reaction ($\sqrt{M} \to \infty$). He noted that his ϕ_a values agree with those of Emmert and Pigford, and he suggested that his data were obtained at long exposure times such as those of Emmert and Pigford, in the range of 0.04 to 0.2 sec. Although no exposure times are reported (3), the liquid flow rates, jet lengths, and approximate jet diameters reported indicate clearly that the exposure time varied from 0.003 to 0.02 sec. Thus the exposure times in Astarita's American experiments are slightly shorter than those in his Italian experiments, and his American data correspond to low values of $\sqrt{M}$ such as those in his Italian experiments and in Clarke's experiments.

Figure 5 shows a comparison of various carbon dioxide–MEA absorption data obtained at 1 atm. It can be seen that Emmert and Pigford's data yield ϕ values is reasonable agreement with Astarita's American data, although the former are for higher values of $\sqrt{M}$. Clarke's data are not shown in Figure 5, but they follow the pseudo first-order curve closely (see Figure 1). In view of the

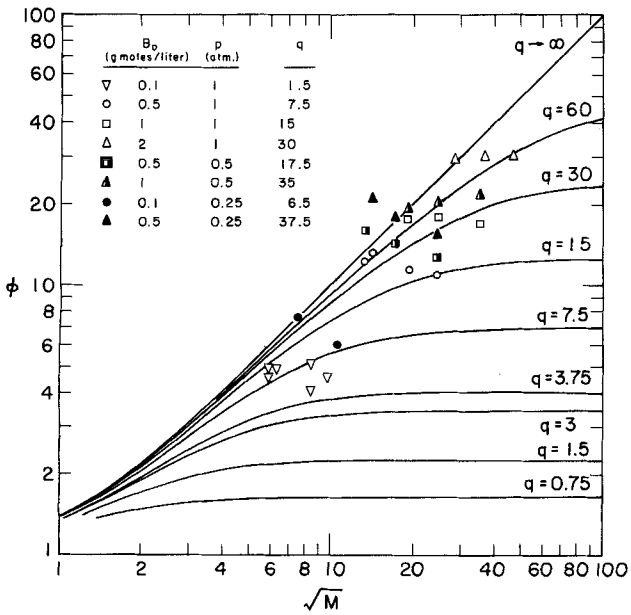

Fig. 3. Emmert and Pigford's data.

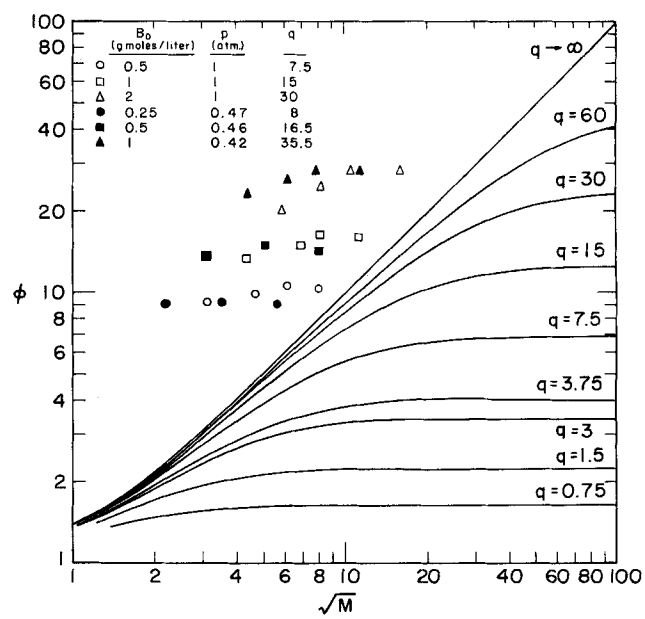

Fig. 4. Astarita's American data.

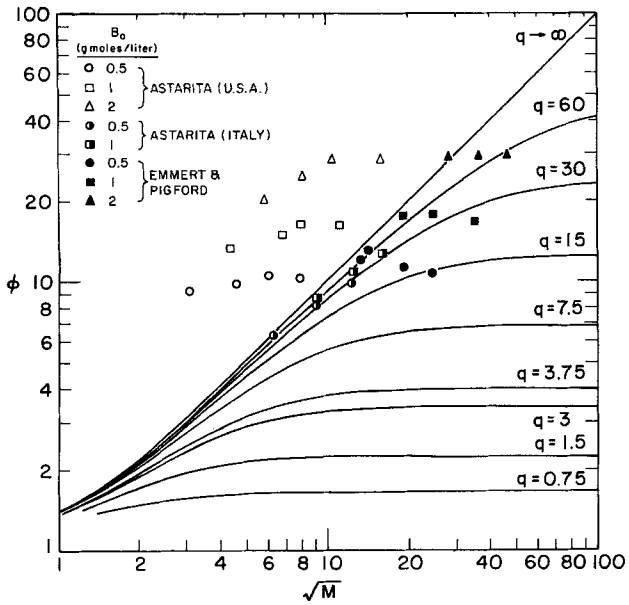

Fig. 5. Comparison of data at $p \simeq 1$ atm.

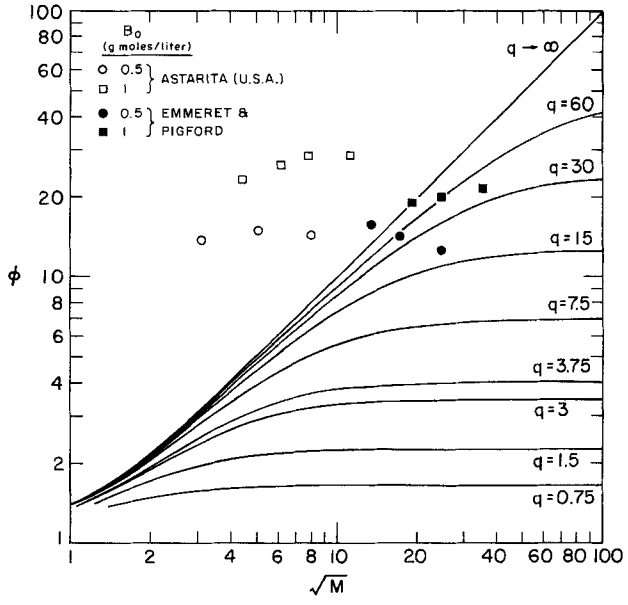

Fig. 6. Comparison of data at $p \simeq 0.5$ atm.

low values of $\sqrt{M}$ for Astarita's American data, they would be expected also to lie near the pseudo first-order curve, rather than to be relatively flat curves at the high ϕ values of Emmert and Pigford's data.

Figure 6 shows a comparison of Emmert and Pigford's data with Astarita's American data for $p = 0.5$ atm. Unlike the situation at 1 atm. the agreement of the levels of the ϕ values here is rather poor.

In the above the carbon dioxide–MEA absorption data available for liquid jets and short wetted-wall columns have been presented and discussed. The general conclusion that can be reached is that most of the data fall above the theoretically predicted values. In addition, there is severe disagreement between the various sets of data. This latter discrepancy can in no way be blamed on the effect of complex chemical kinetics. It must be concluded that the carbon dioxide–MEA absorption system is indeed very poorly understood and that the available data challenge very severely the reliability of classical chemical absorption theory.

Because of the curious behavior of the previously published data on the rate of absorption of carbon dioxide into MEA solutions, this study was undertaken in order to attempt to obtain an understanding of the reasons for this behavior. It was suspected that interfacial turbulence, produced by surface tension gradients, might be responsible for the deviations of the data from theory, even though previous workers reported no visible evidence of such interfacial turbulence. Thus it was decided that the present experiments should include the desorption of an inert tracer simultaneously with the absorption of carbon dioxide into MEA solutions in order to check on the possibility that the chemical absorption process causes a change in the physical mass transfer coefficient.

EXPERIMENT

The experimental program involved the measurement of gas absorption and desorption rates in a short glass wetted-wall column. The device used was similar in design to that of Vivian and Peaceman (*47*) and of Gilliland, Baddour, and Brian (*18*) except for a modification of the gas inlet tube (*24*). This modification was an adaptation of a design of Roberts and Danckwerts (32) and was meant to prevent the formation of stagnant layers on the surface of the liquid film flowing on the glass wall of the column.

Two types of mass transfer measurements were performed. Carbon dioxide was absorbed in water and dilute MEA solutions, while propylene was desorbed from water and MEA solutions. The propylene was used as a tracer in some of the experiments, since its desorption rate was used for inferring the physical transfer coefficient, that is, the fluid mechanics, prevailing during the simultaneous absorption of carbin dioxide into MEA.

The calculation of carbon dioxide absorption coefficients relied on the analysis of outlet liquid samples for carbon dioxide. For carbon dioxide-water absorption this analysis was performed by means of the Winkler method (*44, 22*). In the case of carbon dioxide-MEA absorption the MEA in the liquid sample had to be masked by the addition of an excess of formaldehyde, so that it would not interfere in the Winkler analysis (*23, 24*). The calculation of propylene desorption coefficients depended on both liquid inlet samples and gas outlet samples. The propylene content of both samples was determined by means of a gas chromatograph with a hydrogen flame ionization detector.

The carbon dioxide gas phase partial pressure was varied between 1 and 0.125 atm. by means of nitrogen dilution. The MEA concentration in the liquid was varied between 0.025 and 0.1 M for the carbon dioxide absorption measurements and between 0.025 and 2 M for propylene desorption. In the propylene desorption runs, the propylene partial pressure in equilibrium with the inlet liquid was varied from approximately 0.7 atm. down to half that value in order to be sure that supersaturation and bubble nucleation did not occur. The exposure time range was 0.15 to 0.40 sec. The experimental temperature was usually 25°C.

Additional details about the experimental procedure as well as a summary of the original data may be found in reference *24*.

CARBON DIOXIDE ABSORPTION RESULTS

Figure 7 presents the results for physical absorption of carbon dioxide into water. The ordinate is the physical gas absorption coefficient, corrected for minor variations in diffusivity and column height. The abscissa is the liquid flow rate, corrected for minor variations in liquid viscosity and density (*18*). The upper line represents the prediction of penetration theory and laminar flow theory [see, for example, Equation (2) of reference *18*]. The agreement of these experimental results with the theoretical line is typical of that achieved by previous workers using a short wetted-wall column.

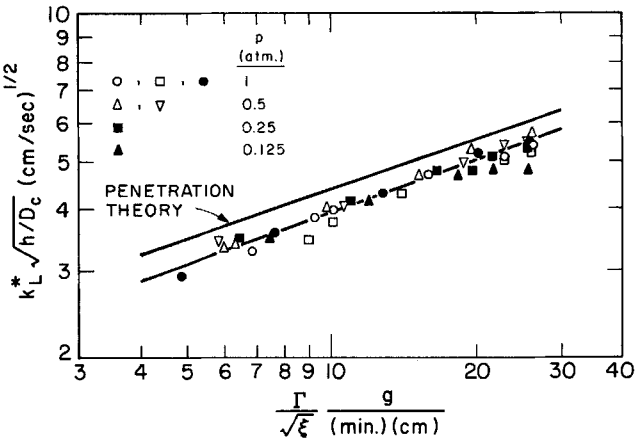

Fig. 7. Physical absorption of carbon dioxide into water.

Figures 8 and 9 present the experimental results for the absorption of carbon dioxide into MEA solutions. Sharma's value of k_F, as given in Table 1, was used in computing $\sqrt{M}$ for each experimental point. Shown for comparison with the experimental results are the same penetration theory curves as those shown in Figures 1 through 6.

The results shown in Figure 8 were obtained at three different partial pressures of carbon dioxide in the gas phase, approximately 1, 0.5, and 0.25 atm. The MEA concentration was also appropriately varied so that $q \equiv B_0/2A_i$ would remain approximately constant at a value of 1.5. It is obvious from Figure 8 that the data do not correlate with each other when the concentration level is changed, despite the fact that q is maintained constant. On this basis alone one could conclude that the data are in disagreement with the theory for a second-order irreversible reaction, which requires that ϕ should obey this correlation. Furthermore, at the two higher concentration levels ϕ decreases at $\sqrt{M}$ increases, and all of the ϕ values exceed the quantitative predictions of the penetration theory. Indeed, the ϕ values at the highest concentration level exceed the theoretical asymptote ϕ_a and would do so even if ν were assumed to be 1 instead of 2. These are the same characteristics observed in the data of Emmert and Pigford, as shown in Figure 3, at higher concentration levels, and they are also observed in the results shown in Figure 9. For $B_o = 0.1$ molar, $p = 1$ atm., it can be seen in Figure 8 that the results of this study are in agreement with the results of Emmert and Pigford.

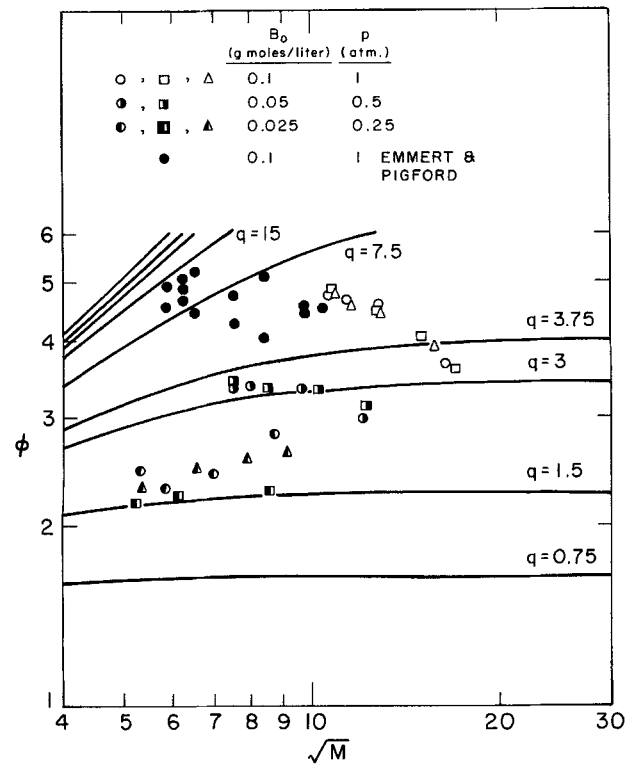

Fig. 8. Carbon dioxide–MEA absorption, $q = 1.5$.

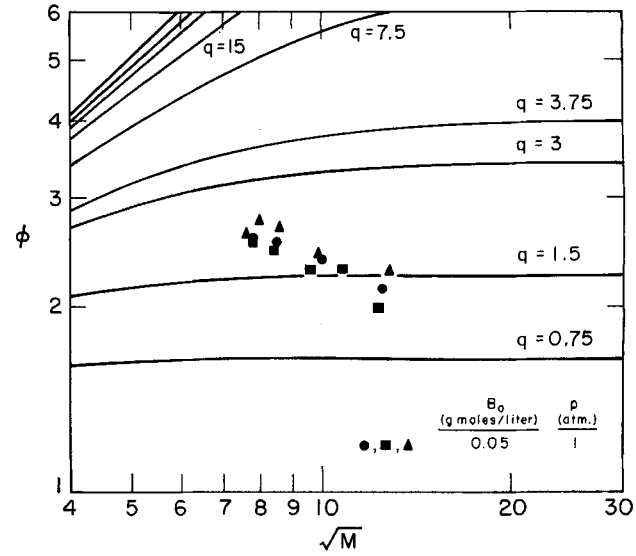

Fig. 9. Carbon dioxide–MEA absorption, $q = 0.75$.

TRACER DESORPTION OF PROPYLENE

Figures 10 and 11 present the propylene desorption coefficient vs. liquid flow rate, plotted in the same manner as the carbon dioxide–water absorption results in Figure 7. The propylene diffusivity used for computing the ordinate values was obtained from Vivian and King (*46*). The dotted lines in Figures 10 and 11 represent the experimental results for carbon dioxide–water physical absorption shown in Figure 7.

Figure 10 reveals that when the gas phase is pure nitrogen ($p = 0$), the propylene desorption coefficient agrees with the carbon dioxide–water physical absorption line whether the liquid phase is pure water or 0.1 molar monoethanolamine. In Figure 11 it is seen that this is also true for desorption of propylene from 1 molar amine solutions into nitrogen gas. Similarly, when propylene is desorbed from pure water into a carbon dioxide gas stream, the desorption coefficient agrees with the carbon dioxide–water physical absorption line, as shown in Figure 10. But when propylene is desorbed from an amine solution into a gas stream containing carbon dioxide, the propylene desorption coefficient lies above the carbon dioxide–water physical absorption line. For example, when propylene is desorbed from a 0.1 molar amine solution into a pure carbon dioxide gas stream at 1 atm., Figure 10 shows that the propylene desorption coefficient exceeds the carbon dioxide–water physical absorption line by a factor of 1.7 at the lowest liquid flow rate and by a factor of 2.3 at the highest liquid flow rate.

Thus it is seen that the chemical absorption of carbon dioxide into MEA alters the propylene desorption coefficient. Since the propylene is an inert tracer at very low concentrations, this is interpreted to mean that the chemi-

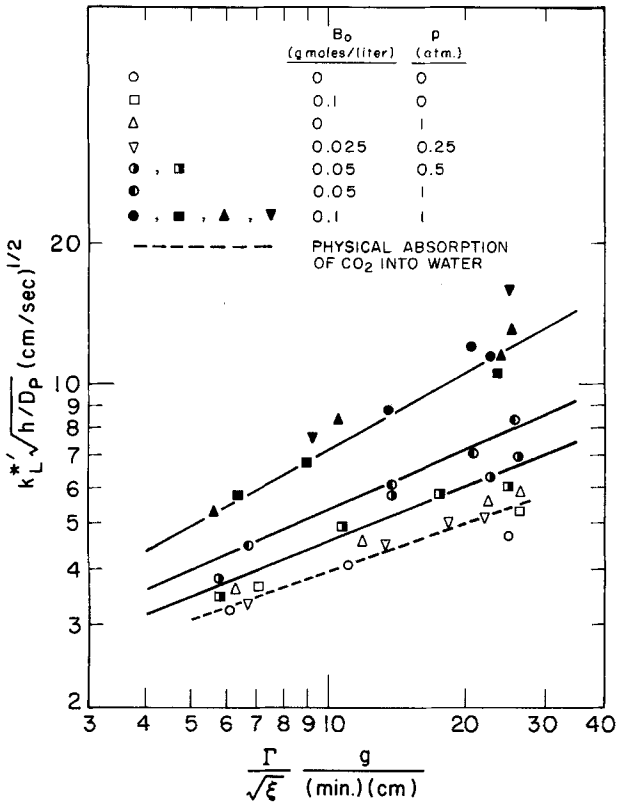

Fig. 10. Propylene desorption.

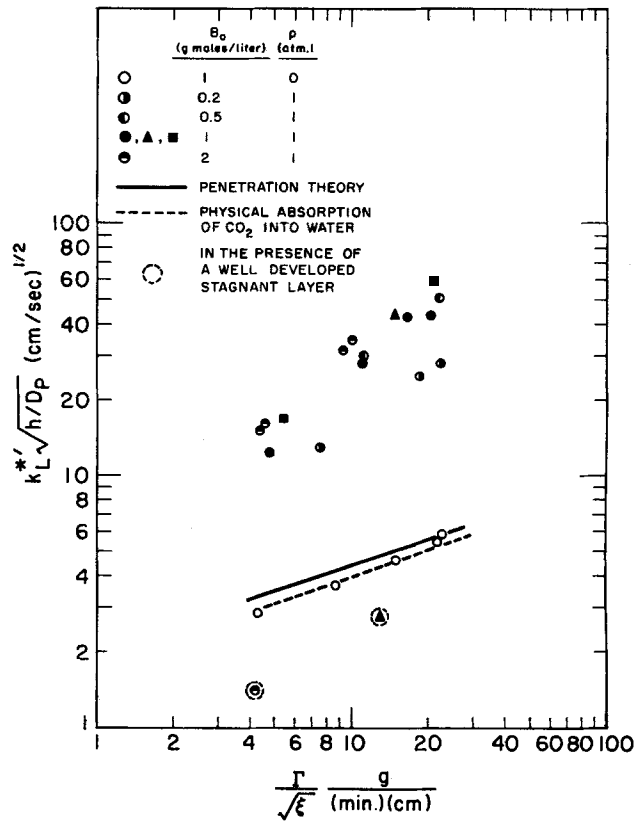

Fig. 11. Propylene desorption.

cal absorption process alters the fluid mechanical nature of the liquid flow in the short wetted-wall column.

Figure 10 reveals that the effect of the carbon dioxide–MEA chemical absorption upon the propylene desorption coefficient increases with amine concentration in the liquid phase and with the carbon dioxide partial pressure in the gas phase, and thus with the carbon dioxide absorption flux. The combinations of B_o and p shown in Figure 10 are the same as those for the carbon dioxide absorption experiments in Figures 8 and 9. At $B_o = 0.025$ molar, $p = 0.25$ atm., Figure 10 shows that the propylene desorption coefficient is not appreciably affected by the chemical absorption process. But at $B_o = 0.1$, $p = 1$, the propylene desorption coefficient has been increased more than twofold.

Figure 11 shows the effect of carbon dioxide–MEA chemical absorption on the propylene desorption coefficient at higher amine concentrations, up to 2 molar, all at $p = 1$ atm. The data for 0.2 molar amine lie appreciably higher than the ones for 0.1 molar amine shown in Figure 10. The desorption coefficient is still higher for 0.5 molar amine, but the coefficient increases only slightly as the amine concentration is further increased to 1 molar and 2 molar. The reason that the propylene desorption coefficient does not continue to increase as the amine concentration increases is that propylene desorption becomes stoichiometrically limited; that is, essentially all of the propylene in the liquid feed is desorbed in the column.

It should be noted that the propylene desorption coefficient is based upon the driving force at the top of the column, and thus it is equal to the desorption flux divided by the propylene concentration in the feed liquid. The carbon dioxide–water physical absorption coefficient is similarly defined in terms of the driving force at the top of the column. This type of definition is the one usually employed, it is consistent with penetration theory ideas, and it is logical for situations in which the concentration change does not penetrate deeply into the liquid layer. But in the present case, this type of definition results in the desorption coefficient approaching a finite asymptote which corresponds to complete removal of the propylene from the liquid. In this case, the concentration change penetrates all the way to the column wall.

Figure 12 shows the propylene desorption results in Figure 11 for $B_o = 0.5$, 1, and 2 molar replotted for comparison with the line (*24*) corresponding to complete removal of the propylene. The agreement of the data with the line in Figure 12 indicates that the stoichiometric limitation is the reason why the propylene desorption coefficient does not continue to increase as B_o

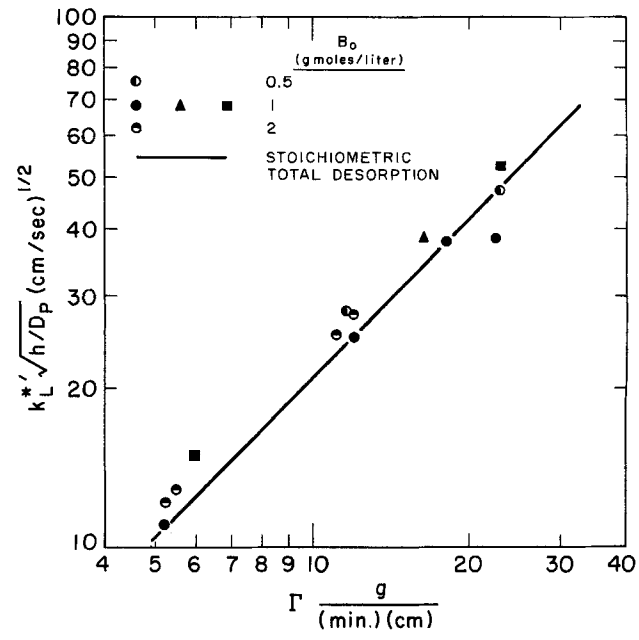

Fig. 12. Propylene desorption at $p = 1$ atm.

is increased beyond 0.5 molar. Because of this, it cannot be concluded that the alteration of the fluid mechanics does not become more severe as B_o is increased beyond 0.5 molar.

The results in Figures 10 and 11 show the dramatic effect of the carbon dioxide–MEA chemical absorption process on the propylene desorption rate. Since the propylene concentration is quite low and the propylene is inert, it would be expected that the propylene desorption process would not affect the carbon dioxide absorption rate, but it was decided that this should be checked experimentally. Thus for one run at $B_o = 0.1$ molar, $p = 1$ atm., represented by ▼ in Figure 10, the carbon dioxide absorption rate was measured in addition to the propylene desorption rate. The resulting carbon dioxide absorption rates are represented by △ in Figure 8, where they can be seen to agree well with the results of two other runs made under the same conditions, except that no propylene was present in the liquid phase. Thus it is concluded that the presence of the propylene did not affect the carbon dioxide absorption rate.

The effect of the carbon dioxide–MEA chemical absorption process on the propylene desorption coefficient indicates a change of the fluid mechanics and more specifically the onset of some kind of turbulence or mixing, which is absent under normal conditions, such those prevailing while carbon dioxide is being absorbed by water. It is suspected that what is involved is interfacial turbulence driven by surface tension gradients. This phenomenon has long been known in liquid-liquid extraction (*27, 28, 39*). For example, Sherwood and Wei (*39*) observed a violent disruption of the interface during liquid-liquid extraction with simultaneous chemical reaction. The interfacial turbulence was quite visible and produced a spray of droplets of the organic phase into the aqueous phase. But in the carbon dioxide–MEA chemical absorption system no visible disturbance of the gas-liquid interface was noted during previous investigations (*1*, 3 to 5, *11*, *14* to *16*) or during the present study, and thus the tracer desorption technique was used to detect the presence of interfacial disturbances. Recent theoretical analyses (*30*, *33* to *35*, *40*, *41*) of interfacial instabilities caused by surface tension gradients suggest that the cellular circulations that result can be very small, and thus there appears to be no reason to doubt the existence of interfacial disturbances just because they are not readily detected by eye. Nevertheless, it would be desirable to develop a photographic technique, perhaps using Schlieren photography, to observe the interfacial disturbances indicated by the tracer desorption studies for the carbon dioxide–MEA system.

REINTERPRETATION OF CARBON DIOXIDE-MEA ABSORPTION

The carbon dioxide–MEA chemical absorption results presented in Figures 8 and 9 were calculated by using the physical transfer coefficient obtained from the carbon dioxide–water physical absorption experiments. In view of the fact that a different physical transfer coefficient prevails during carbon dioxide–MEA absorption, as can be seen from Figure 10, this procedure is unjustified. A better method would be to use the propylene desorption coefficient obtained for the same liquid flow rate, carbon dioxide partial pressure, and MEA concentration. This has been done in Figures 13 and 14, where the results are expressed as ϕ' vs. $\sqrt{M'}$. The prime indicates that the propylene desorption coefficient $k_L^{*\prime}$ has been used as the physical absorption coefficient in calculating these two quantities. It can be seen in Figures 13 and 14 that the agreement between the experimental results and the

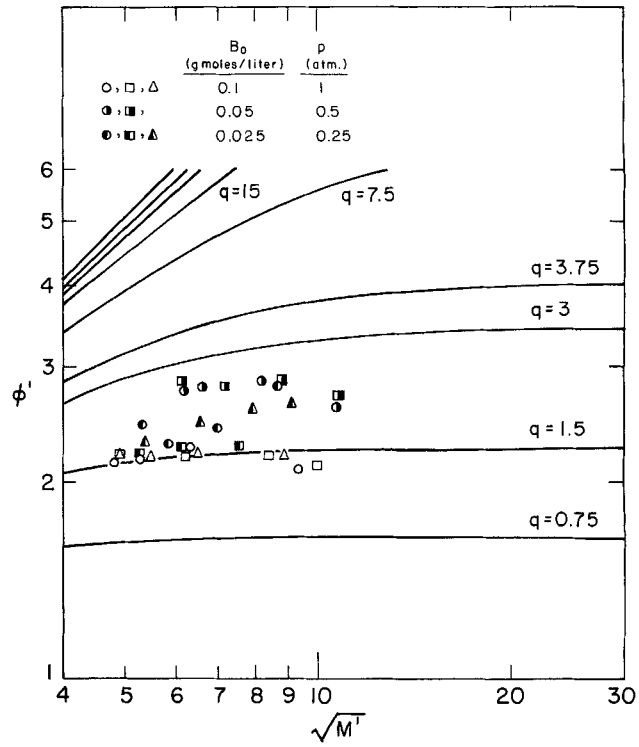

Fig. 13. Reinterpretation of carbon dioxide–MEA absorption, $q = 1.5$.

theoretical curves is considerably improved by using the new calculation procedure, but the agreement is not perfect. Of course the curves represent penetration theory, while the experimental results were obtained under conditions where the physical transfer coefficient was augmented by the interfacial turbulence; thus the applicability of these theoretical curves to this experimental situation is certainly questionable.

When the diffusivity ratio r is equal to unity, theoretical ϕ vs. $\sqrt{M}$ curves for rather different fluid mechanical models (*10, 13, 17, 26, 29, 38, 43, 45*) show surprising agreement with each other; thus there is some reason to hope that penetration theory curves can be applied to

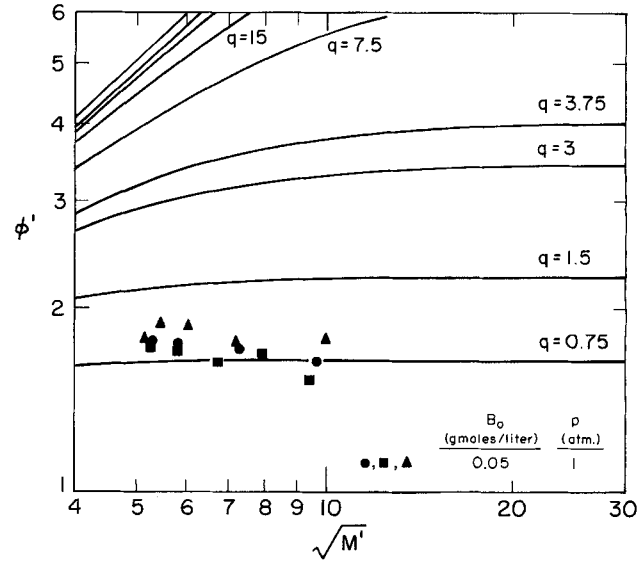

Fig. 14. Reinterpretation of carbon dioxide–MEA absorption, $q = 0.75$.

an experimental situation in which the fluid mechanics differ from the penetration theory idealization. But when $r = 0.573$ as in the carbon dioxide–MEA system, different models do show appreciably different results. Furthermore, if different regions of the gas-liquid surface possess different physical transfer coefficients due to more or less interfacial turbulence, it is possible that the average value of ϕ for the entire surface might deviate from the theoretical curves even if these curves applied accurately to each region of surface separately, because of the nonlinear nature of the curves. Finally, when the interfacial turbulence becomes so great that the propylene concentration change penetrates to the column wall and the propylene desorption rate becomes stoichiometrically limited, the value of $k_L^{*\prime}$ becomes insensitive to further increases in the intensity of the turbulence, as discussed earlier. But the carbon dioxide–MEA chemical absorption rate would continue to increase with increased interfacial turbulence, and in this range the use of $k_L^{*\prime}$ to correct the results would not be meaningful. Thus the $k_L^{*\prime}$ values in Figure 11 cannot be used for a meaningful reinterpretation of the results of Emmert and Pigford (*14* to *16*). In view of the above considerations, the deviation of the corrected experimental results from the penetration theory curves in Figures 13 and 14 is not wholly unexpected.

The physical gas absorption coefficient appears to the first power in the denominator of both ϕ and $\sqrt{M}$. Thus, the procedure adopted for correcting the results for interfacial turbulence resulted in dividing both of these variables by the same quantity $k_L^{*\prime}/k_L^*$. On a logarithmic plot of ϕ vs. $\sqrt{M}$ this correction resulted in moving each experimental point down along a 45-deg. line toward lower ϕ and $\sqrt{M}$ values. Since the uncorrected ϕ vs. $\sqrt{M}$ values lie above the theoretical curves in Figures 8 and 9, the corrected values lie much closer to the theoretical curves, as shown in Figures 13 and 14. Furthermore, Figure 10 reveals that $k_L^{*\prime}/k_L^*$ increases with concentration level at a given value of q, and thus the correction procedure tends to bring together the results at a given value of q, as seen by comparing Figures 8 and 13. The correction factor $k_L^{*\prime}/k_L$ is also a function of liquid flow rate, and thus the correction procedure eliminates the decrease in ϕ as $\sqrt{M}$ increases. This is especially apparent in comparing the results for $B_o = 0.1$ molar, $p = 1$ atm. in Figures 8 and 13.

Since the pseudo first-order curve closely approaches a 45-deg. line for $\phi > 3$, and since the correction procedure shifts the experimental points down along a 45-deg. line, ϕ vs. $\sqrt{M}$ points which agree with the pseudo first-order line will continue to agree with it after being corrected to ϕ' vs. $\sqrt{M'}$. Therefore the fact that Clarke's results agree with the pseudo first-order curve, as shown in Figure 1, does not necessarily imply that interfacial turbulence was not causing an increase in the physical mass transfer coefficient. Indeed, if ϕ' and $\sqrt{M'}$ are substantially reduced from ϕ and $\sqrt{M}$, this could explain why Clarke's results agree with the pseudo first-order curve instead of falling below it as the large values of $\sqrt{M}$ would seem to require. On the other hand, Astarita's American data lie above the pseudo first-order curve, as shown in Figure 4. Therefore, if the correction procedure is to bring these results into agreement with the theoretical curves, the data points would have to be corrected all the way down to the point where the pseudo first-order curve departs from the 45-deg. line. This would require a correction factor $k_L^{*\prime}/k_L^*$ between 8 and 20 for the data points shown in Figure 4. This does not seem unreasonable in view of the $k_L^{*\prime}/k_L^*$ values shown in Figure 11.

It was seen earlier that previously obtained carbon dioxide–MEA data show disagreements from investigator to investigator. This could be due to the intensity of interfacial turbulence varying from one experimental system to another, perhaps because of different contact times, different curvatures of the liquid surface, or different surface-active impurities present in the system.

The deviations from theory reported for chlorine desorption from water by Peaceman (*29*) and Kniel (*21*) and for chlorine absorption into acidified aqueous ferrous chloride solutions by Gilliland, Baddour, and Brian (*18*) involve excessively high mass transfer rates at the higher concentration levels. This behavior is sufficiently similar to that observed here that is reasonable to conclude that these two systems might also involve interfacial turbulence during chemical absorption.

STAGNANT LAYER FORMATION

It was found in the present investigation that a stagnant layer may build up in the short wetted-wall column and cover part of the surface of the liquid film. This phenomenon has been observed by other investigators (*25*, *32*, *12*) and it is very likely due to surfactant accumulation. The two encircled points in Figure 11 were obtained in the presence of well-developed stagnant layers covering most of the surface of the film. It can be seen that a very significant reduction of the propylene desorption rate is caused by the stagnant layer. Other experiments (*24*) indicate that the carbon-dioxide–MEA absorption rate is also reduced when a stagnant layer is covering the film. One would expect (*24*) that the effect of the stagnant layer would be especially large for systems involving interfacial turbulence. It is possible that the disagreement among previous carbon dioxide–MEA investigations is partly due to the stagnant layer formation tendency to vary from one experimental system to the other. It should be emphasized that all of the present data reported here, with the exception of the two encircled points in Figure 11, were obtained in the absence of a stagnant layer.

CONCLUSION

Previously published experimental data on the rate of absorption to carbon dioxide into aqueous MEA solutions deviate seriously from penetration theory predictions for gas absorption accompanied by a second-order chemical reaction. Furthermore, the experimental results show disturbing disagreements when one investigation is compared with another. The results of the present study indicate that these deviations are due to interfacial turbulence, presumably produced by surface tension gradients during the chemical absorption process. The interfacial turbulence is not readily visible, but its presence was detected by desorbing the inert tracer propylene simultaneously while carbon dioxide was being absorbed into MEA. The substantial increase in the propylene desorption coefficient indicated the presence of the interfacial turbulence and served as a measure of its intensity. When the carbon dioxide–MEA absorption results were reinterpreted by using the actual physical mass transfer coefficient prevailing, as indicated by the propylene desorption coefficient, the carbon dioxide–MEA data showed much better, although not perfect, agreement with penetration theory.

It appears likely that other chemical absorption systems, such as chlorine desorption from water and chlorine absorption into ferrous chloride solutions, may involve interfacial turbulence. This suggests the need for tracer desorption studies to accompany all fundamental investigations of simultaneous gas absorption and chemical reac-

tion. Finally, since interfacial turbulence is probably present in commercial gas absorbers as well as in laboratory absorbers, but since its intensity appears to vary considerably, the need for studies leading to a better understanding of the production of the interfacial turbulence is apparent.

ACKNOWLEDGMENT

Financial support from the National Science Foundation, Socony Mobil Oil Company, and from an Esso Research and Engineering Company fellowship (to D. C. Matiatos) is gratefully acknowledged. The assistance of Professor J. D. Sherman with the analysis of propylene and of Dr. P. G. Laux of Vulcan-Cincinnati, Inc., with the analysis of carbon dioxide in the presence of MEA is gratefully acknowledged. D. C. Matiatos is indebted to Dr. Theodore Schoenberg for many helpful suggestions.

NOTATION

A = carbon dioxide concentration in the liquid phase, g.-moles/liter

B = monoethanolamine concentration in the liquid phase, g.-moles/liter

D_c = liquid phase diffusion coefficient for carbon dioxide, sq. cm./sec.

D_M = liquid phase diffusion coefficient for monoethanolamine, sq. cm./sec.

D_p = liquid phase diffusion coefficient for propylene, sq. cm./sec.

h = height of short wetted-wall column, cm.

k_F = reaction rate constant as defined by Equation (2), liters/(g.-mole) (sec.)

k_L = liquid phase gas absorption coefficient for carbon dioxide in the presence of the carbon dioxide–MEA chemical reaction, cm./sec.

k_L^* = physical gas absorption coefficient for normal hydrodynamics in column, cm./sec.

$k_L^{*\prime}$ = physical gas absorption coefficient, as indicated by propylene desorption rate, for actual hydrodynamics prevailing during carbon dioxide–MEA absorption, cm./sec.

$\sqrt{M} = \sqrt{\left(\frac{\pi}{4}\right) k_F B_o t}$ for penetration theory

$= \sqrt{k_F D_c B_o}/k_L^*$ for experimental results

$\sqrt{M'} = \sqrt{k_F D_c B_o}/k_L^{*\prime}$

p = gas phase partial pressure of carbon dioxide, atm.

$q = B_o/\nu A_i$

$r = D_M/D_c$

T = temperature, °C.

t = time of exposure of liquid to gas, sec.

Greek Letters

Γ = liquid flow rate per unit of column perimeter, g./(min.) (cm.)

ν = stoichiometric coefficient, moles of reacting solute per mole of transferring species, = 2 for carbon dioxide–MEA according to Equation (1)

ξ = product of the liquid density and viscosity divided by the same product for water at 25°C.

$\phi = k_L/k_L^*$

$\phi' = k_L/k_L^{*\prime}$

ϕ_a = asymptotic value of ϕ as $\sqrt{M} \to \infty$

Subscripts

i = gas-liquid interface

o = feed (or bulk) liquid

LITERATURE CITED

1. Astarita, Gianni, *Chem. Eng. Sci.*, **16**, 202 (1961).
2. ———, *Chim. Ind.*, **42**, 849 (1960).
3. ———, M.Ch.Eng. thesis, Univ. Delaware, Newark (1960).
4. ———, *R. C. Acad. Napoli S4*, **27**, 176 (1960).
5. ———, *Ric. Sci.*, **30**, 658 (1960).
6. ———, G. Marrucci, and F. Gioia, *Chem. Eng. Sci.*, **19**, 95 (1964).
7. ———, *Rend. Sci. Fis. Mat. Nat. Accad. Lincei*, **34**, 176 (1963).
8. Brian, P. L. T., *A.I.Ch.E. J.*, **10**, 5 (1964).
9. ———, and M. C. Beaverstock, *Chem. Eng. Sci.*, **20**, 47 (1965).
10. Brian, P. L. T., J. F. Hurley, and E. H. Hasseltine, *A.I.Ch.E. J.*, **7**, 226 (1961).
11. Clarke, J. K. A., *Ind. Eng. Chem. Fundamentals*, **3**, 239 (1964).
12. Cullen, E. J., and J. F. Davidson, *Trans. Faraday Soc.*, **53**, 113 (1957).
13. Danckwerts, P. V., and A. M. Kennedy, *Trans. Inst. Chem. Engrs.*, **32**, S49 (1954).
14. Emmert, R. E., Ph.D. thesis, Univ. Delaware, Newark (1954).
15. ———, and R. L. Pigford, *A.I.Ch.E. J.*, **8**, 171 (1962).
16. *Ibid.*, 702.
17. Friedlander, S. K., and M. Litt, *Chem. Eng. Sci.*, **7**, 229 (1958).
18. Gilliland, E. R., R. F. Baddour, and P. L. T. Brian, *A.I.Ch.E. J.*, **4**, 223 (1958).
19. Himmelblau, D. M., *Chem. Rev.*, **64**, 545 (1954).
20. Jensen, M. B., E. Jørgensen, and C. Faurholt, *Acta Chem. Scand.*, **8**, 1137 (1954).
21. Kniel, K., S.B. thesis, Massachusetts Inst. Technol., Cambridge (1951).
22. Laitinen, H. A., "Chemical Analysis," p. 96, McGraw-Hill, New York (1960).
23. Laux, P. G., Private communication, Vulcan-Cincinnati, Inc., Cincinnati, Ohio (1964).
24. Matiatos, D. C., Sc.D. thesis, Massachusetts Inst. Technol., Cambridge (1965).
25. Merson, R. L., and J. A. Quinn, *A.I.Ch.E. J.*, **11**, 391 (1965).
26. Olander, D. R., *ibid.*, **6**, 233 (1960).
27. Orell, Aluf, and J. W. Westwater, *Chem. Eng. Sci.*, **16**, 127 (1961).
28. ———, *A.I.Ch.E. J.*, **8**, 350 (1962).
29. Peaceman, D. W., Sc.D. thesis, Massachusetts Inst. Technol., Cambridge (1951).
30. Pearson, J. R. A., *J. Fluid Mech.*, **4**, 489 (1958).
31. Perry, J. H., "Chemical Engineers' Handbook," 4 ed., Chap. 14, p. 17, McGraw-Hill, New York (1963).
32. Roberts, D., and P. V. Danckwerts, *Chem. Eng. Sci.*, **17**, 961 (1962).
33. Ruckenstein, E., and C. Berbente, *ibid.*, **19**, 329 (1964).
34. Scriven, L. E., and C. V. Sternling, *Nature*, **187**, 186 (1960).
35. ———, *J. Fluid Mech.*, **19**, 321 (1964).
36. Sharma, M. M., Ph.D. thesis, Univ. Cambridge, England (1964).
37. ———, and P. V. Danckwerts, *Chem. Eng. Sci.*, **18**, 729 (1963).
38. Sherwood, T. K., and J. M. Ryan, *ibid.*, **11**, 81 (1959).
39. Sherwood, T. K., and J. C. Wei, *Ind. Eng. Chem.*, **49**, 1030 (1957).
40. Smith, K. A., *J. Fluid Mech.*, **24**, 401 (1966).
41. Sternling, C. V., and L. E. Scriven, *A.I.Ch.E. J.*, **5**, 514 (1959).
42. Thomas, W. J., and I. A. Furzer, *Chem. Eng. Sci.*, **17**, 115 (1962).
43. Toor, H. L., and S. H. Chiang, *A.I.Ch.E. J.*, **5**, 339 (1959).
44. Treadwell, F. P., and W. T. Hall, "Analytical Chemistry," 9 ed., Vol. 2, p. 498, Wiley, New York (1942).
45. Vieth, W. R., J. H. Porter, and T. K. Sherwood, *Ind. Eng. Chem., Fundamentals*, **35**, 1 (1963).
46. Vivian, J. E., and C. J. King, *A.I.Ch.E. J.*, **10**, 220 (1964).
47. Vivian, J. E., and D. W. Peaceman, *ibid.*, **2**, 437 (1956).

Manuscript received February 4, 1966; revision received May 31, 1966; paper accepted June 2, 1966